



Open  
Access

## Response of Viscous Damping of Dashpot Containing Hybrid Nanofluid

Hayder Abdul khaliq Ali<sup>1</sup>, Mayyadah S. Abed<sup>2,\*</sup>, Adil Abed Nayeeif<sup>1</sup>

<sup>1</sup> Department of Mechanical Engineering, Mustansiriyah University, Baghdad, Iraq

<sup>2</sup> Department of Materials Engineering, University of Technology, Iraq

### ARTICLE INFO

#### Article history:

Received 31 October 2019

Received in revised form 16 December 2019

Accepted 16 December 2019

Available online 15 March 2020

### ABSTRACT

This work aimed to enhance the viscous damping of the oil shock absorbers by adding (1,2,3,4,5) vol% of single-phase fumed silica or precipitated silica to the hydraulic oil. Hybrid phases were also used (functionalized MWCNT and fumed silica) as 5 vol% as total volume fraction adding. Nanofluid was prepared by using Ultrasonic Probe Sonicator. The effect of different additive concentrations of nano structure to the pure hydraulic oil of dashpot (damper) was tested by the free damping vibration rigid body beam apparatus. The decayed in amplitude cycles are recorded by pen recorder at the free end of the rigid beam. Damping coefficients, maximum overshoot and settling time for both kinds of nanofluid was calculated. Comparative study was investigated among the damping coefficient responses respect with each other. The obtained results indicate that the energy dissipated by viscous damping friction was decreased at different concentrations of nanostructure (single-phase and hybrid) dispersed in oil of the apparatus dashpot. The single-phase of 5 vol% MWCNTs and 0% of silica (OS5C) exhibits significant enhancement in response specifications and steady-state (such as maximum overshoot and settling time) of the rigid beam body. Due to the different behavior during damping test, rheological properties were also investigated for the hybrid nanofluid to sense and explain the damping results.

#### Keywords:

Nano-fluid; MWCNTs; Free and Forced  
Vibration of Rigid-Body; logarithmic  
decrement

Copyright © 2020 PENERBIT AKADEMIA BARU - All rights reserved

## 1. Introduction

Vibration is one of the most popular issues in industries that cause acoustic pollution, machine heating, wearing of fixtures, fatigue etc. creates many causes for failure. Due to these problems, damping of vibrations is the solution which deals with a wide range of engineering applications such as designing the building, vehicle suspensions, aerospace etc.

Recently, nanotechnology has significant attention to treat like these obstacles. Nanotechnology is a field which describes and manipulates the properties of materials at the nanoscale, to develop the applications in science, engineering and medicine [1]. These materials could be metals like nanosilver, ceramics like carbon nanotubes and graphene [2-4], or polymer and nanocomposites [5].

\* Corresponding author.

E-mail address: [11038@uotechnology.edu.iq](mailto:11038@uotechnology.edu.iq) (Mayyadah S. Abed)

Nanofluid is a newly discovered field which deals with many areas. This work focuses on nanofluid which acts as a vibration damper.

N D Sims *et al.*, utilized smart fluids (electrorheological (ER) and magnetorheological) in vibration damping devices under proportional feedback control. Nonlinear force/velocity characteristic of the resulting damper is significantly observed [6]. M. Nabeel Rashin *et al.*, prepared novel eco-friendly ZnO-coconut oil nanofluid in various concentrations ultrasonically. The viscosity had been determined at different temperatures and shear rates. The shear-thinning behaviour is noticed in all samples. The shear-thinning was significantly high at low shear rates and high adding content [7]. E. Etefaghi *et al.*, facilitated different nanostructures additives (multi-walled carbon nanotubes and oxides) with various concentrations dispersed in SAE 20W50 engine oil to improve lubricant properties. The results showed a significant effect on viscosity, flash point, pour point and thermal conductivity coefficient of engine oil [8, 9]. Mohammad Hemmat Esfe *et al.*, determined thermal conductivity and rheology of silver-magnesium oxide/water hybrid nanofluid to investigate the effect of nanoparticle volume fraction on these properties with the particle diameter 40 nm for (50 vol% MgO) and 25 nm for (50 vol% Ag) nm ranging between 0% -2% [10]. Fang-Yao Yeh *et al.*, invented a micro-nano fluid damper, which can absorb and transform the vibration to thermal energy to be dissipated, and effectively enhances the viscosity and thermal conduction of the micro-nano fluid, thereby having better result of impact absorption [11]. Mohammad Hemmat Esfe *et al.*, studied the rheology of Al<sub>2</sub>O<sub>3</sub>/engine oil nanofluid in various vol% and temperatures. The volume fractions were 0.25%, 0.5%, 0.75%, 1%, 1.5% and 2% at temperature range 5 - 65 °C. The results showed that the nanofluid viscosity increased with the additives vol%. Also, it had been found that viscosity of nanofluid decreases with increasing temperature [12]. Xianqian Wu *et al.*, determined the dynamic behaviour of sandwich panels filled partially with STF using the modified split Hopkinson pressure bar (SHPB) apparatus. The stresses versus strain curves are plotted to determine the energy absorption of the material composite [13]. Ali Alirezaie *et al.*, investigated the rheological behaviour of COOH-MWCNT / MgO - Engine oil hybrid nanofluid [14]. Kamran Sepyani *et al.*, evaluated the effect of ZnO nanoparticles on the rheological behaviour of engine oil [15]. Haider Nadhom Azziz *et al.*, investigated the Ag-Nano lubricant effect on air conditioning performance [16]. Mohammad Hashemian *et al.*, prepared viscous fluid containing CNTs and studied the nonlocal dynamic stability of carbon nanotubes subjected to axial harmonic load by Bolotin's method [17]. Other researchers reviewed the damping properties and rheological characteristics for different types of nano additives impregnated in suitable fluids as single or hybrid phases [18,19].

In the present work, some underlying assumptions are taken into account to facilitate system modelling such as the beam as a rigid – body and non-deformable under the action of the external forces, also assume a linear system analysis by reducing the parameters that illustrated the translation and rotation of the rigid beam body system [20] and excludes the bodies that display highly elastic, and plastic behaviour. Another one, using the most straightforward mathematical treatment to measure the amount of present damping indicated by the rate of decay of oscillation called logarithmic decrement. The suitable changing of system dashpot oil properties done by mixing it with the different concentrations of nanostructures (fumed silica, precipitated silica and functionalized Multi-walled carbon nanotubes MWCNT-COOH). The present work aimed to investigate the effect of the nanofluid at the dashpot oil damping coefficient and the corresponding position of the dashpot itself. The damping coefficient is estimated as logarithmic decrement, determined by amplitude decay of the beam free vibration.

## 2. Theory

The system illustrated in Figure 1 is a system of free vibration damping of a rigid body beam, as shown in this figure the left end of the rigid beam fixed by a turn-on pivoted (ball bearings located in a fixed housing), where the right end supported by spring (stiffness). This spring bolted to the bracket, and the later fixed to the top member of the rig structure which enables beam end to raise and lowering to get a fine adjustment. The exciter motor bolted rigidly to the beam with two unbalanced discs on the shaft provides an additional load to the system. The trace paper pen recorder fixed at the right end of the vertical frame and consists of a rotating drum at law constant speed is driven by a synchronous motor, operated speed control device. The pen tip fits the free end of the rigid beam and adjustment so that the pen just touches the paper. This allows recording the cycles number performed by the rigid beam smoothly each time. The kinematic and kinetics is described the angular motion and the acceleration of the rigid body beam system which can be represented as a function of time.

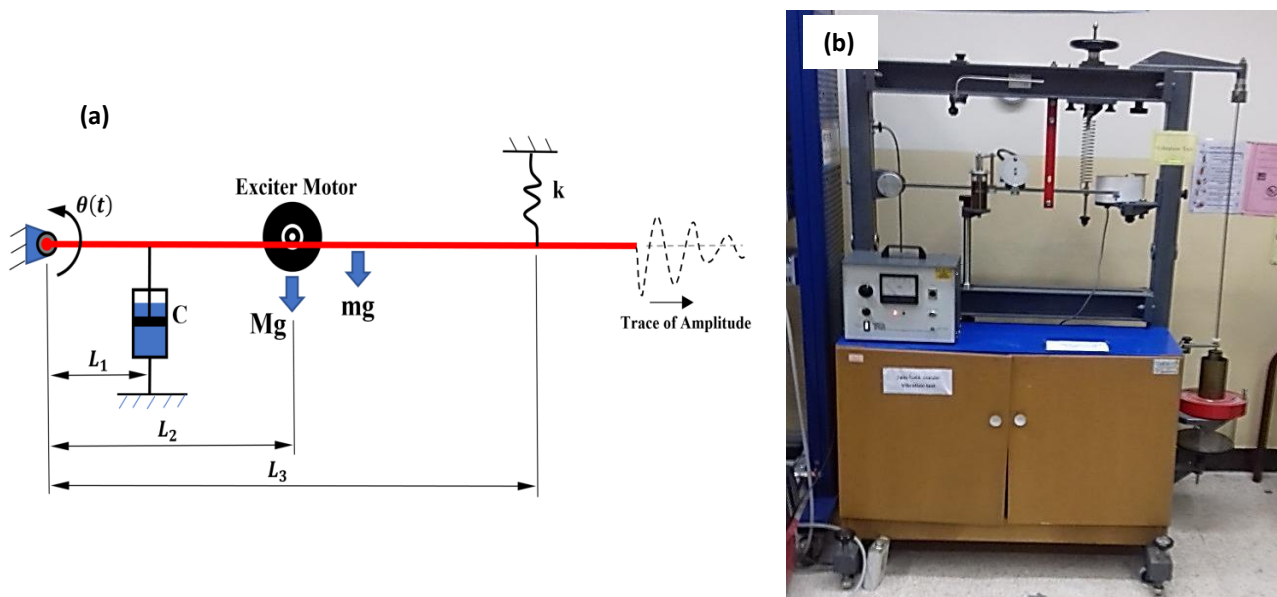


**Fig. 1.** (a) Schematic diagram of free damping rigid body – beam vibration system, (b) TQ Universal Vibration Apparatus

The equation of the angular motion as it indicated in [20]:

$$\ddot{\theta}(t) + \alpha \dot{\theta}(t) + b\theta(t) = 0 \quad (1)$$

$$\text{Where: } = \frac{CL_1^2}{I_A}, \quad b = \frac{kL_3^2}{I_A}.$$

$$\text{and } I_A \approx ML_2^2 + \frac{mL^2}{3}$$

$\theta$  = angular displacement of the rigid body beam. The angular equation of motion (1) can be arranged according to the standard form of the second-order system as follows:

$$\ddot{\theta} + 2\zeta\omega_n \dot{\theta}(t) + \omega_n^2 \theta(t) = 0 \quad (2)$$

In this paper, Laplace transformation was used with initial condition  $\theta(0) = a_o$ ,  $\dot{\theta}(0) = 0$  instead of time-domain analysis as in [21], and the same calculation were founded as in the damped vibration period and the logarithmic decrement equation respectively. Know the equation of angular motion becomes:

$$[s^2\Theta(s) - sa_o] + 2\zeta\omega_n [s\Theta(s) - a_o] + \omega_n^2 \Theta(s) = 0 \quad (3)$$

$$(s^2 + 2\zeta\omega_n s + \omega_n^2)\Theta(s) = (s + 2\zeta\omega_n)a_o \quad (4)$$

$$\Theta(s) = a_o \frac{s+2\zeta\omega_n}{s^2+2\zeta\omega_n s+\omega_n^2} \quad (5)$$

$$= a_o \frac{s+\zeta\omega_n+\zeta\omega_n}{s^2+2\zeta\omega_n s+\zeta^2\omega_n^2-\zeta^2\omega_n^2+\omega_n^2} \quad (6)$$

$$= a_o \frac{s+\zeta\omega_n}{(s+\zeta\omega_n)^2+\omega_d^2} + \frac{\zeta\omega_n}{(s+\zeta\omega_n)^2+\omega_d^2} \quad (7)$$

$$= a_o \left[ \frac{s+\zeta\omega_n}{(s+\zeta\omega_n)^2+\omega_d^2} + \frac{\zeta}{\sqrt{1-\zeta^2}} \frac{\omega_d}{(s+\zeta\omega_n)^2+\omega_d^2} \right] \quad (8)$$

$$\theta(t) = a_o e^{-\zeta\omega_n t} \left[ \cos\omega_d t + \left( \frac{\zeta}{\sqrt{1-\zeta^2}} \right) \sin\omega_d t \right] \quad (9)$$

The solution of the equation of motion becomes:

$$\theta(t) = a_o e^{-\zeta\omega_n t} \cos(\omega_d t - \phi_1) \quad (10)$$

Let  $t_1$  and  $t_1$  refers to the time corresponding to two amplitudes  $x_0$  and  $x_1$  (displacement), determined one cycle apart for an under-damped system using the above equation. We can form the ratio,

$$\frac{\theta(t_1)}{\theta(t_2)} = \frac{a_o e^{-\zeta\omega_n t_1} \cos(\omega_d t_1 - \phi_1)}{a_o e^{-\zeta\omega_n t_2} \cos(\omega_d t_2 - \phi_2)} \quad (11)$$

But  $t_2 = t_1 + \tau$  where  $\tau = \frac{2\pi}{\omega_d}$  is the damped vibration period, knowing the above equation as:

$$\frac{x(t_1)}{x(t_2)} = \frac{e^{-\zeta\omega_n t_1} \cos(\omega_d t_1 - \phi_1)}{e^{-\zeta\omega_n(t_1+\tau)} \cos(\omega_d(t_1+\tau) - \phi_1)} \quad (12)$$

$$\frac{x_0}{x_1} = \frac{e^{-\zeta\omega_n t_1}}{e^{-\zeta\omega_n t_1} e^{-\zeta\omega_n \tau}} = e^{\zeta\omega_n \tau} \quad (13)$$

Then, the logarithmic decrement is:

$$\delta = L_n \frac{x_0}{x_1} = \zeta\omega_n \tau \quad (14)$$

$$\zeta = \frac{\delta^2}{\sqrt{(2\pi)^2 + \delta^2}} \quad (15)$$

From the standard form of a second-order system, where

$$2\zeta\omega_n = \frac{C}{M} \tag{16}$$

$$C = 2\zeta\omega_n \tag{18}$$

$\zeta$  : damping ratio.

### 3. Experiments

#### 3.1 Materials Used

A functionalized Multiwalled carbon nanotube was purchased from United Nanotech Innovations PVT. LTD, which prepared by chemical vapour deposition method CVD and then further treated to introduce –COOH group to be suitable for organic solvents. Chemical analysis and discretion of this product is illustrated in Tables 1 and 2. Surface morphology had been done in this work facilitating transmission electron microscope TEM (type JEOL 1400, USA, with accelerating voltage 40–120 kV, magnification 50X–800,000X), and scanning electron microscope SEM (Hitachi S-4700- HRSEM, Japan, accelerating voltage 0.5-30 kV, and resolution of 1.5 nm). Fumed silica (functionalized with –OH group) was supplied from Guangzhou GBS High-Tech and Industry Co., Ltd. (see Table 3). Whereas precipitated silica (Vilkasil C) was purchased from Bayer Company (see Table 4). Scanning electron microscope SEM was utilized to characterize the surface morphology of fumed and precipitated silica. Commercial hydraulic oil was provided from the local market (see Table 5).

**Table 1**  
 Chemical Analysis, value expressed in mass percentage

Carbon	Oxygen	Hydrogen	Sulphur	Chlorine	Trace metal	Ash
> C72 %	> 20 %	> 6 %	<1%	1%	<0.01%	<0.1%

**Table 2**  
 MWCNTs Description

MWCNT	Description
Production method	Chemical vapor Deposition
Available form	Black powder
Diameter	Outer diemetr:20-40 nm
Length	<10 $\mu$ m
Nanotubes purity	>9%
Metal particles	< 2%
Amorphous carbon	< 1%
Specific surface area	212 m <sup>2</sup> /g
Extent of carboxylation	>10%

**Table 3**  
 Properties of fumed silica

Property	Details/Value
Appearance	White colloidal powder
Sp. Surface area (m <sup>2</sup> /g)	388
pH	4.12
Loss on drying at 105°C (%)	0.56
Loss on ignition at 1000°C (%)	1.02
Tamped density (g/l)	43

Silica content (%)	99.88
Carbon content (%)	0.1
Chloride content (%)	0.011
Other oxides (%)	0.013
Thixotropic index	6.87

**Table 4**  
 Properties of precipitated silica (Vulkasil C)

Property	Details/Value
Appearance	Fine agglomerate white powder
Water content (Wt.%)	10 - 14
Surface area (m <sup>2</sup> /g)	<u>45 - 65</u>
Sp.gr.	1.95
Particle size (nm)	20 - 25
Agglomerate particle size (µm)	2 - 15
Thermal conductivity (W/m. °C)	1.4

**Table 5**  
 Commercial oil used characteristics

Property	Details/Value
SAE viscosity grade	50
Caterpillar Test	TO-4
Allison Test	C-4
ISO Viscosity Grade	----
Gravity API (ASTM D287)	24.7
Flash point °C (°F) (ASTM D92)	240 (464)
Pour point °C (°F) (ASTM D97)	-15 (5) min
Viscosity	
cP at -25°C (ASTM D5293)	----
cSt at 40°C (ASTM D445)	195
cSt at 100°C (ASTM D445)	18.0
Viscosity Index (ASTM D2270)	96
Calcium, %wt.	0.298
Zinc, %wt (ASTM D4951)	0.127
Phosphorous, % wt. (ASTM D4951)	0.11
Sulfated ash, % wt. (ASTM D4951)	1.2

### 3.2 Nano Fluid Preparation

The nanofluid mixture was designed according to the volume fraction percentage as illustrated in Table 6. Functionalized Multi-Walled Carbon Nanotubes (C), fumed silica (FS) and precipitated silica (PS) are dispersed into liquids of dashpot oil (Hydraulic) by using ultrasonication probe Type Qsonica 2000 watt, England at mixing condition (40% Intensity, 1s:1s pulse/off period of pluses, 10 min mixing time at 30 °C) as shown in Figure 2. The prepared nanofluid samples are shown in Figure 3.

**Table 6**  
 Single and hybrid phases nanofluid mixture design

Code	Precipitated silica (PS) Vol%	Code	Fumed silica (FS) Vol%	Code	Fumed silica Vol%	CNTs Vol%
0	0	0	0	0	0	0
1PS	0	1FS	0	5S0C	5	0
2PS	1	2FS	1	4S1C	4	1
3PS	2	3FS	2	3S2C	3	2

4PS	3	4FS	3	2S3C	2	3
5PS	4	5FS	4	1S4C	1	4



**Fig. 2.** The ultrasonicator probe



**Fig. 3.** The nanofluid samples; (a) Fumed silica nanofluid, (b) Precipitated silica nanofluid, (c) Carbon nanotube nanofluid

### 3.3 Vibration Damping Test

The rigid body beam of free damping vibration system as shown in the previous Figure 1 consist of a rectangular cross-section and dashpot with viscous friction damping effects are used to suppression the free vibration of the rigid beam system. Dispersed different concentration of nanoparticles in hydraulic oil to study the effect of these concentrations on the decay of the amplitude then will be calculated the damping parameters corresponding to dashpot location. The following procedure illustrated the experimental work of the present paper. At the beginning keeps the end of beam moving to equilibrium position (i.e. horizontal beam) by adjustments spring to set the right end of the rigid beam at the equilibrium position. Fixed the damper at distance  $L_1$  which is from pivot to the centre of the dashpot beam clamp so that this damper is perpendicular with the

clamp beam (respectively, after each change in the dashpot location. The beam must be adjustment horizontally). When pen recorder contacts trace paper to record the cycles number of at the constant speed of drum per unit time (3 sec) or the damping frequency of the rigid beam. When the time of stopwatch end turn off the switch of the speed control device after pulling down the free right end of the rigid beam at a short distance (10 mm) and releasing. For each recording of cycles per previous time, vary the dashpot location and its clamps along the length of a rigid beam by choosing different values of  $L_1$  such as (0.1, 0.15, 0.2, and 0.25 in meter). From the chart recorder, the logarithmic decrement can be obtained from an amplitude ratio  $\left(\frac{x_0}{x_1}\right)$ , which is measured by Eq. (14). Now the period time of single complete oscillation is:

$$\tau = (3 \text{ sec.}) \left(\frac{\tau_1}{\tau_2}\right) \quad (18)$$

Where  $\tau_1$  : is the distance between two frequencies.

$\tau_2$  : is the total distance of the pen recorder for 3 sec.

Also, to find the damping coefficient (C) and natural frequency of free damping vibration of a rigid beam system, the Eq. (14) and Eq. (15) meet the requirements.

### 3.4 Rheology Test

Rheology test was executed to determine the viscosity through a wide average speed 200-1000 rpm. This test was done utilizing Brookfield viscometer (DV-II+Pro) at room temperature. The viscosity was recorded when the value fixed after a period of time. The hybrid nanofluid was selected to test for all concentration when was noticed different behavior of some concentration during damping.

## 4. Results and Discussion

Surface morphology of used CNT was characterized by TEM and SEM images as shown in Figures 4 and 5. Outer diameter (20-40 nm) of CNT is with average length  $< 10 \mu\text{m}$ . SEM images of fumed and precipitated silica are shown in Figures 6 and 7. It seems that fumed silica have average size 20-59 nm whereas precipitated silica with average size 20-25 nm.

Figure 8 showed the result of rheology test of hybrid nanofluid for all concentrations (0S5C, 1S4C, 2S3C, 3S4C, 5S0C). It can be observed significantly the shear thickening behaviour of all concentration but this behaviour be clearer when the CNT% be higher.

The results obtained from the present work of the rigid beam of free damping vibration system needed to make some calculations such as the time for one cycle (period of vibration) when switching off the stopwatch, the logarithmic decrement and the corresponding frequency with damping coefficient by using the Eq. (14) to Eq. (17). The value of the moment of inertia can be found with using Eq. (1). Table 7 illustrates the parameters of the rigid beam free damping vibration system.

The experiment results showed the magnitudes of oscillations due to free vibrations in simple structures and how damping affects their vibrations. Comparing these results of a pen recorder trace paper to evaluate the logarithmic decrement vibration for oil of the dashpot with those simulated in MATLAB program for both pure hydraulic oil and (0S5C) as in Figures 9 and 10. In these two figures, the sample was taken of the many results made in the present work. The amplitude ratio of both pure ( $x_{o\_exp} = 11\text{mm}$ ,  $x_{1\_exp} = 9\text{mm}$ ,  $x_{o\_th} = 13.5\text{mm}$ ,  $x_{1\_th} = 11\text{mm}$ ) and the additive concentration

(0S5C) ( $x_{o\_exp} = 11.5\text{mm}$ ,  $x_{1\_exp} = 8\text{mm}$ ,  $x_{o\_th} = 13.2\text{mm}$ ,  $x_{1\_th} = 9.2\text{mm}$ ) respectively. The comparison was made by placing the practical oscillation curve as the background of the simulation curve on a similar scale. The response error between (0S5C) and pure hydraulic oil are 12.8% and 18.5% respectively.

**Table 7**  
 Rigid beam of free damping vibration system parameters

Parameter	Value
Mass of motor with discs, M	4.102kg
Mass of beam, m	2kg
Lengths, $L_1$	(0.05, 0.1, 0.15, 0.2, 0.25, 0.3, 0.35)m
Lengths, $L_2$	45cm
Length, $L_3$	63cm
Length, $L_4$	73cm

Figure 11 (a, b) indicated that the two curves (1FS and 1PS) were closed to the pure hydraulic oil curve. This shows that the well-dispersed of both fumed silica (FS) and precipitated silica (PS) in hydraulic oil decreases the damping coefficient of rigid beam when subjected to free vibration. In laboratory experiments, the location of the dashpot away from the fixed end (pivoted end) of rigid beam leading to increase the torsional damping force and damping coefficient increases. When comparing the results obtained from the two curves 1FS and 1PS with pure hydraulic oil curve as in Figure 11, curve 1PS was found to be slightly better than 1FS curve. This effect is attributed to the shear thinning of nanofluid when added silica at all concentration [9].

Also, damping coefficients of single-phase nanofluids (fumed or precipitated silica with pure hydraulic oil) at different volume% (1PS, 2PS, 3PS, 4PS, 5PS) and (1FS, 2FS, 3FS, 4FS, 5FS) were illustrated in Figure 12 (a, b) respectively. Whereas hybrid nanofluid contains fumed silica (S) and CNT (C) at different volume% (1S4C, 4S1C, 2S3C, 3S2C, 5S0C, and 0S5C) is shown in Figure 13. It was noted that adding silica (fumed or precipitated) decreases the damping ratio gradually with increasing adding vol% of particles. So, adding the silica with CNTs, the decreasing was also noticed with fluctuating behaviour depending on which material takes control of fluid behaviour. But when incorporated with only CNT (0S5C), the well homogenized and functionalized CNT with oil increases the damping ratio of pure hydraulic oil. Figure 14 shows the different behaviour of damping between higher adding vol% of CNT (0S5C), and fumed silica (5S0C), these results agreed with the researchers [8,9].

When CNTs are incorporated into the oil, they are placed between oil layers and lead to ease of slippage and moving of fluid layers on each other, and viscosity will slightly decrement. Whereas when concentration increases, nanotubes agglomerate and prevent the movement of oil layers on each other; so, the viscosity will increment. The shear-thickening will be the viscosity control at higher concentration of CNTs, which be approved in rheology test. In reality, viscosity change in nanofluid affected by different factors such as kind of fluid, kind of nanoparticles, nanoparticles concentration, and the dispersion method [8].

Observing the results in Figure 15, it can be seen the damping enhancement significantly as present of maximum overshoots (MP%) at the first cycle of oscillation curve for (0S5C) relative with (5S0C) and pure hydraulic oil.

The response curve of free damping vibration of rigid beam at (0S5C) concentration was reached to steady state faster than other concentrations as shown in Figure 16, in this figure the various concentrations has closely rate change of settling time (fast response) vs changes in damping coefficient corresponding to pure hydraulic oil, except the additive concentrations of MWCNT-COOH

as clearly shown in Figure 17, an improvement occurs in settling time when comparing the results of both (0S5C) and (5S0C) corresponding to pure hydraulic oil due to an increases in damping coefficient. But the additive concentrations (1S4C) and (4S1C) causes an increase in settling time of system response (i.e. long time to reach to steady-state) due to decreasing in damping coefficient as in Figure 18. Similarly, the concentrations (2S3C) and (3S2C) made adverse responses of the free damping vibration of rigid body beam system as in Figure 19 [11].

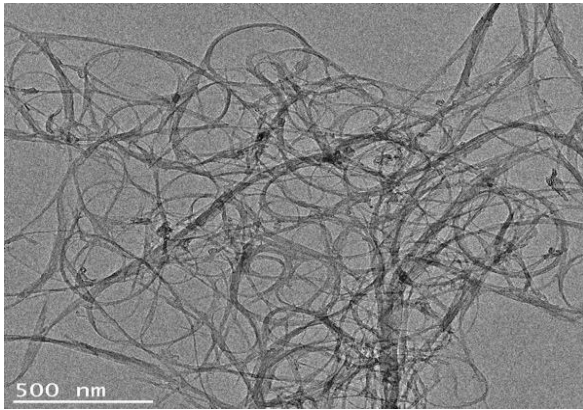


**Fig. 4.** TEM image of MWCNT

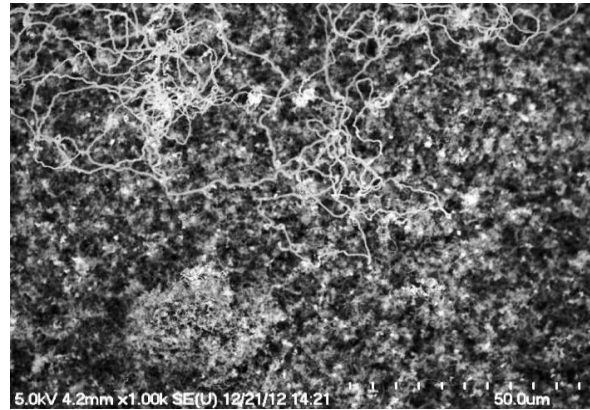


**Fig. 5.** SEM image of MWCNT

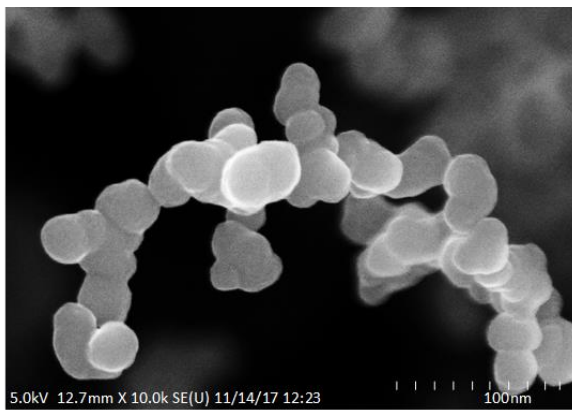


**Fig. 6.** SEM image of fumed silica

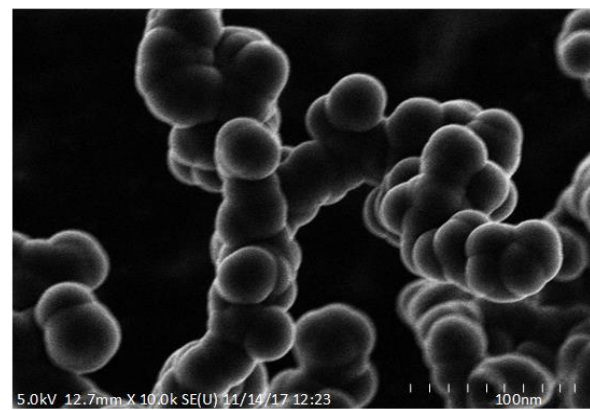


**Fig. 7.** SEM image of precipitated silica

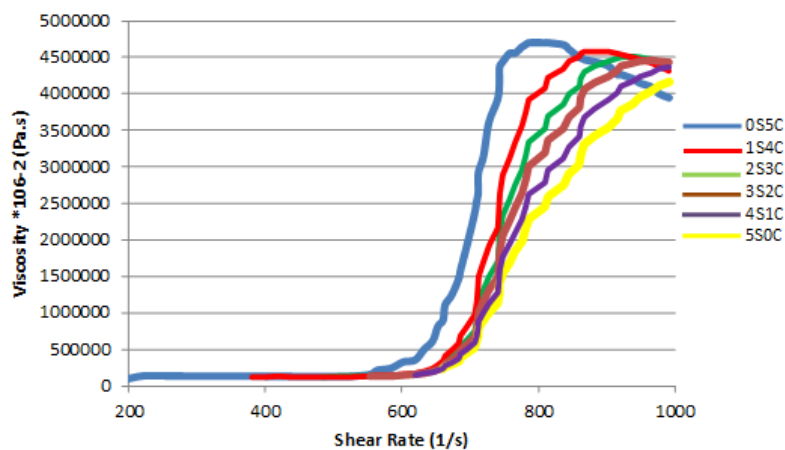


**Fig. 8.** Viscosity versus shear rate of hydride nanofluid at different concentrations

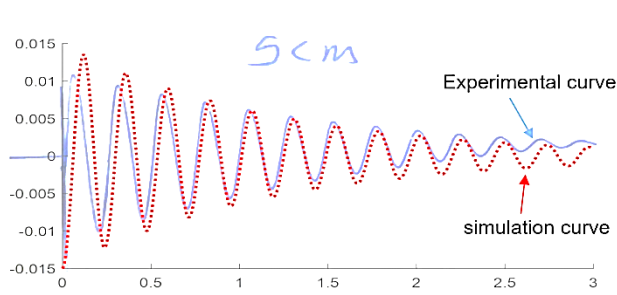


**Fig. 9.** Simulated the experimental result of damping response for pure hydraulic oil at 5 cm distance

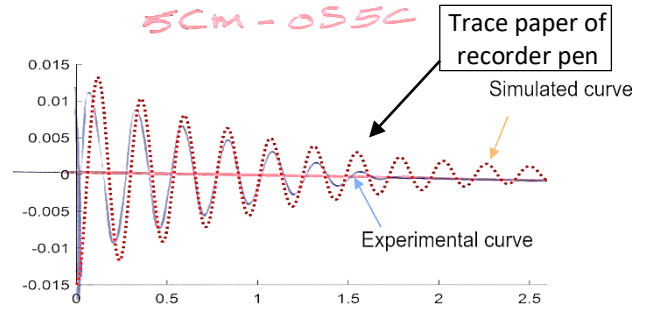


**Fig. 10.** Simulated the experimental result of damping response for (OS5C) at 5 cm distance

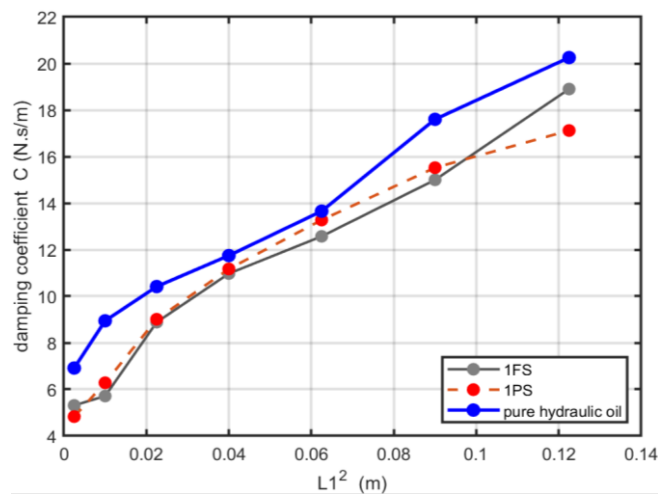


**Fig. 11.** Comparison of damping coefficients responses between 1 Vol% of fumed silica (1FS) and precipitated silica (1PS) corresponding to pure hydraulic oil

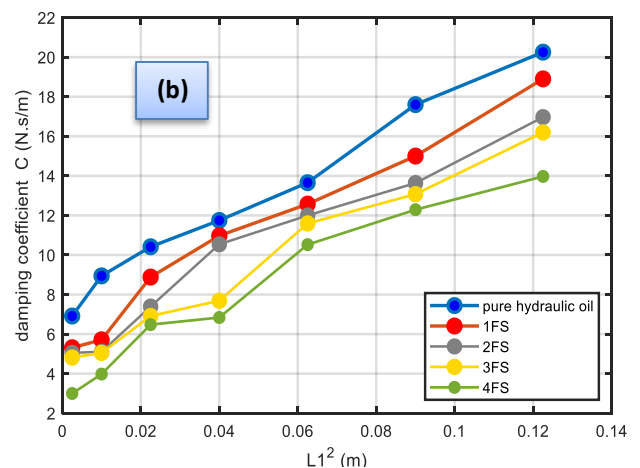
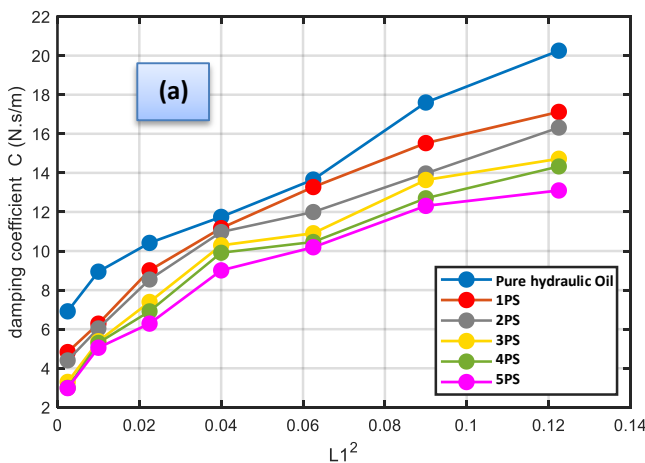


**Fig. 12.** Damping coefficient responses of single phase nanofluid containing (a) fumed silica (FS), (b) precipitated silica (PS), at different Vol%

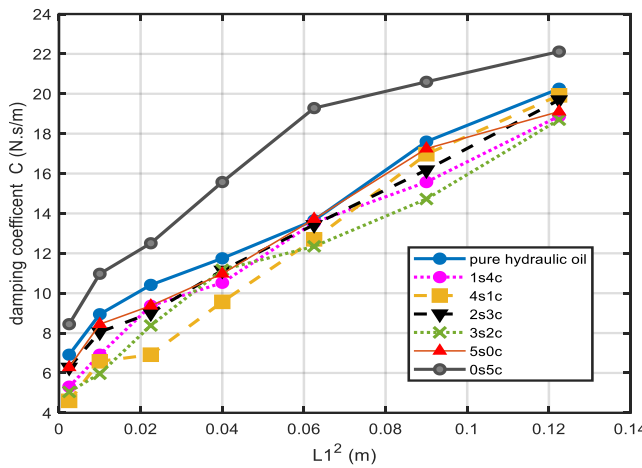


**Fig. 13.** Damping coefficient responses for hybrid Nano-fluid (Fumed silica +MWCNT) at different Vol%

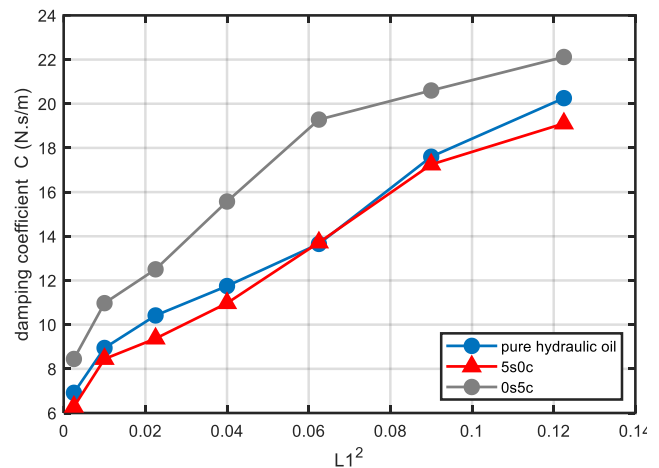


**Fig. 14.** Comparison of damping coefficient responses of (5S0C) vs (0S5C) corresponding to pure hydraulic oil

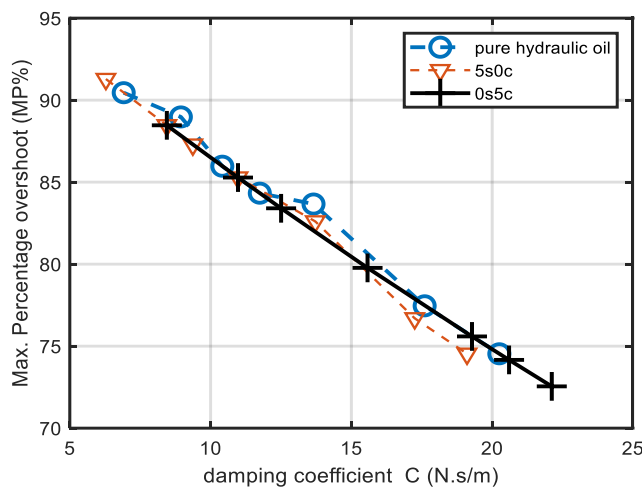


**Fig. 15.** Max. % overshoot versus damping coefficient of (5S0C) vs (0S5C) corresponding to pure hydraulic oil

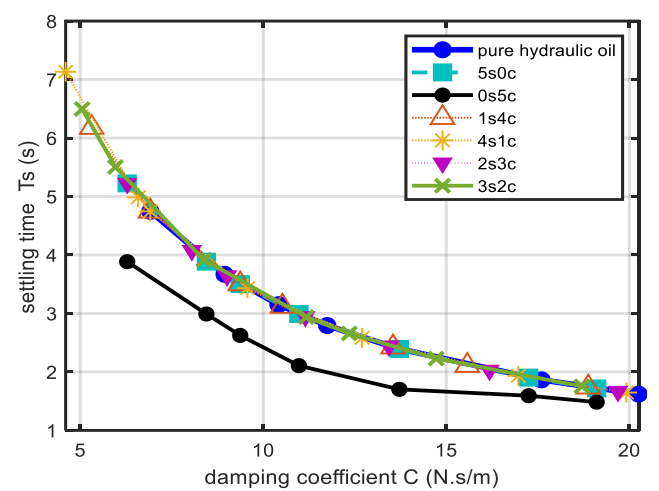


**Fig. 16.** Settling time versus damping coefficients of various concentrations

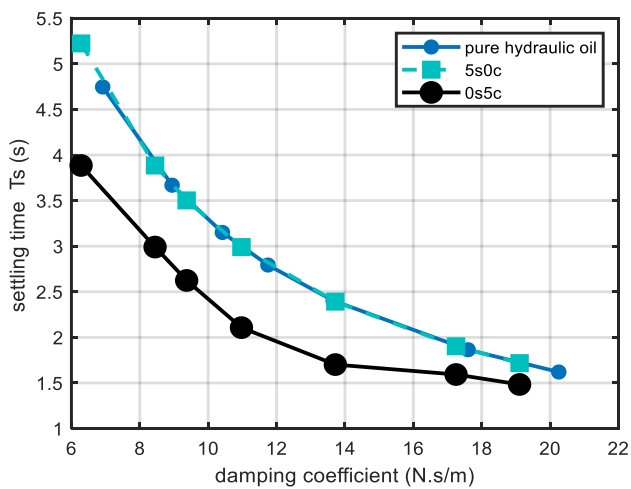


**Fig. 17.** Settling time corresponding damping coefficient of (5S0C) and (0C5S)

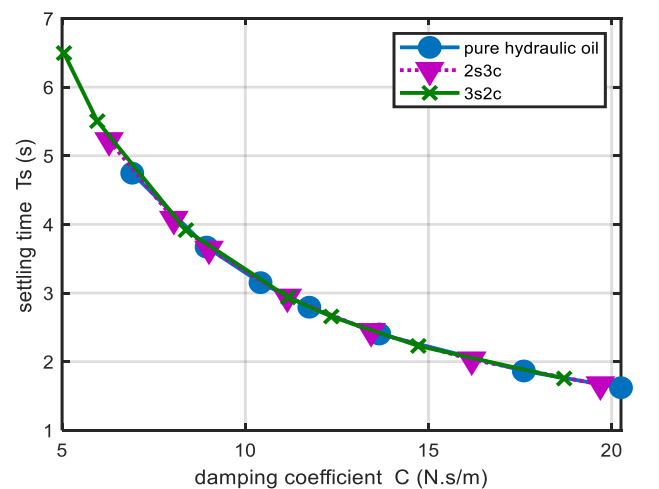


**Fig. 18.** Settling time corresponding damping coefficient of (1S4C) and (4S1C)

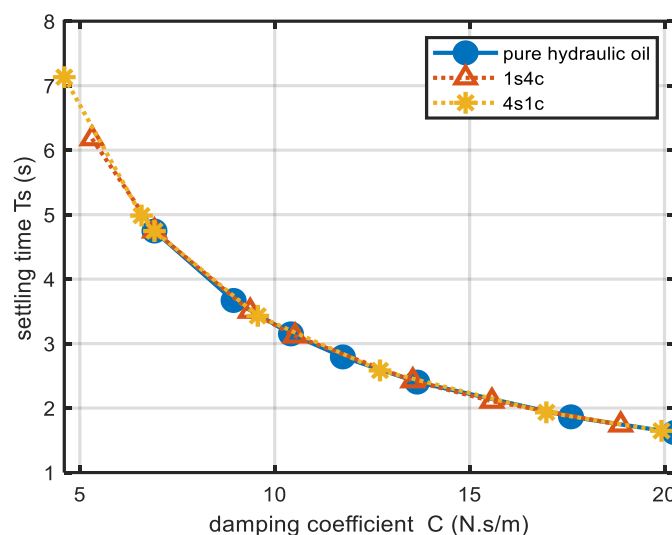


**Fig. 19.** Settling time corresponding damping coefficient of (2S3C) and (3S2C)

## 5. Conclusion

Single-phase and a hybrid nanofluid damper is prepared by ultrasonicated different volume fraction from the functionalized carbon nanotubes and silica (fumed and precipitated) in pure hydraulic oil. The damping results showed the different behaviour under test. It could be concluded the different behaviour of the damping coefficient and settling time of nanofluid is due to the attributing the matter kind, shape, surface modification and shear thickening and thinning hypothesis. The vibration energy dissipated by viscous damping friction decreased when nanostructures additives were dispersed in dashpot oil (single-phase and hybrid) at all concentrations. Single-phase of 5 vol% MWCNTs and 0% of silica (0S5C) exhibits significant enhancement in response specifications and steady-state (such as maximum overshoot and settling time) of the rigid beam body. These results approved by rheology test when the shear thickening behavior of fluid is significantly observed at a higher concentration of CNTs. Finally, it can be concluded that adding MWCNTs to hydraulic oil has no appreciable effect on viscosity at low concentrations.

## References

- [1] Lidén, Göran. "The European commission tries to define nanomaterials." *Annals of Occupational Hygiene* 55, no. 1 (2011): 1-5.
- [2] Abed, Mayyadah Shanan, Ashwaq S. Abed, and Farhad Mohammad Othman. "Green Synthesis of Silver Nanoparticles from Natural Compounds: Glucose, Eugenol and Thymol." *Journal of Advanced Research in Fluid Mechanics and Thermal Sciences* 60, no. 1 (2019): 95-111.
- [3] Abed, Mayyadah S. "Preparation and Characterization of Carbon Nanotubes Composite." PhD thesis Department of Materials Engineering/University of Technology-Iraq (2014).
- [4] Abed, Mayyadah S. "Preparation of graphene nanoribbons (GNRs) from twisted structure carbon nanotubes using unzipping technique." In *IOP Conference Series: Materials Science and Engineering*, vol. 454, no. 1, p. 012159. IOP Publishing, 2018.
- [5] Adnan Hamad, Qahtan, and Mayyadah S. Abed. "Investigation of Thyme and Pumpkin Nanopowders Reinforced Epoxy Matrix Composites." *Journal of Mechanical Engineering Research & Developments* 42, no. 5 (2019): 153-157.
- [6] Sims, N. D., R. Stanway, D. J. Peel, W. A. Bullough, and A. R. Johnson. "Controllable viscous damping: an experimental study of an electrorheological long-stroke damper under proportional feedback control." *Smart materials and structures* 8, no. 5 (1999): 601.
- [7] Rashin, M. Nabeel, and J. Hemalatha. "Synthesis and viscosity studies of novel ecofriendly ZnO-coconut oil nanofluid." *Experimental Thermal and Fluid Science* 51 (2013): 312-318.

- [8] Ettefaghi, Ehsan-o-llah, Hojjat Ahmadi, Alimorad Rashidi, Amideddin Nouralishahi, and Seyed Saeid Mohtasebi. "Preparation and Thermal Properties of Oil-Based Nanofluid from Multi-Walled Carbon Nanotubes and Engine Oil as Nano-Lubricant." *International Communications in Heat and Mass Transfer* 46 (2013): 142–147.
- [9] Ettefaghi, Ehsan-o-llah, Rashidi, Alimorad, Hojjat Ahmadi, Seyed Saeid Mohtasebi, and Mahnaz Pourkhalil. "Thermal and Rheological Properties of Oil-Based Nanofluids from Different Carbon Nanostructures." *International Communications in Heat and Mass Transfer* 48 (2013): 178–182.
- [10] Esfe, Mohammad Hemmat, Masoud Afrand, Samira Gharehkhani, Hadi Rostamian, Davood Toghraie, and Mahidzal Dahari. "An experimental study on viscosity of alumina-engine oil: effects of temperature and nanoparticles concentration." *International Communications in Heat and Mass Transfer* 76 (2016): 202-208.
- [11] Yeh, Fang-Yao, Kuo-Chun Chang, Tsung-Wu Chen, and Chung-Han Yu. "Micro-nano fluid damper." U.S. Patent 9,422,997, issued August 23, 2016.
- [12] Esfe, Mohammad Hemmat, Ali Akbar Abbasian Arani, Mohammad Rezaie, Wei-Mon Yan, and Arash Karimipour. "Experimental Determination of Thermal Conductivity and Dynamic Viscosity of Ag–MgO/water Hybrid Nanofluid." *International Communications in Heat and Mass Transfer* 66 (2015): 189–195.
- [13] Wu, Xianqian, Qiuyun Yin, Chenguang Huang, and Fachun Zhong. "Dynamic energy absorption behavior of lattice material filled with shear thickening fluid." *Procedia engineering* 199 (2017): 2514-2518.
- [14] Alirezaie, Ali, Seyfolah Saedodin, Mohammad Hemmat Esfe, and Seyed Hadi Rostamian. "Investigation of rheological behavior of MWCNT (COOH-functionalized)/MgO-engine oil hybrid nanofluids and modelling the results with artificial neural networks." *Journal of Molecular Liquids* 241 (2017): 173-181.
- [15] Sepyani, Kamran, Masoud Afrand, and Mohammad Hemmat Esfe. "An experimental evaluation of the effect of ZnO nanoparticles on the rheological behavior of engine oil." *Journal of Molecular Liquids* 236 (2017): 198-204.
- [16] Azziz, Haider Nadhom, Abbas Sahi Shareef, and Hadeel Salah Hadi. "Experimental Investigation of the Ag-Nano Lubricant Effect on Air Conditioning Performance." *Journal of Advanced Research in Fluid Mechanics and Thermal Sciences* 61, no. 1 (2019): 147-154 .
- [17] Hashemian, Mohammad, Amir Homayoun Vaez, and Davood Toghraie. "Investigation of viscous fluid flow and dynamic stability of CNTs subjected to axial harmonic load coupled using Bolotin's method." *International Journal of Numerical Methods for Heat & Fluid Flow* (2019).
- [18] Oh, Jong-Seok, and Seung-Bok Choi. "A Review on the Development of Dampers Utilizing Smart Magnetorheological Fluids." *Current Smart Materials* 4, no. 1 (2019): 15-21.
- [19] Ibrahim, Haziqatulhanis, Norazlianie Sazali, Ahmad Syahiman Mohd Shah, Mohamad Shaiful, Abdul Karim, Farhana Aziz, and Wan Norharyati Wan Salleh. "A Review on Factors Affecting Heat Transfer Efficiency of Nanofluids for Application in Plate Heat Exchanger." *Journal of Advanced Research in Fluid Mechanics and Thermal Sciences* 60, no. 1 (2019): 144-154.
- [20] Universal Vibration Apparatus Catalogue TMO1PC.
- [21] Rao, Singiresu S. "Mechanical Vibrations.[SI]." *Pearson Education* (2011).